Noise properties in the Nagel-Schreckenberg traffic model

Shu-ping Chen and Ding-wei Huang
Department of Physics, Chung Yuan Christian University, Chung-li, Taiwan
(Received 6 November 2000; published 21 February 2001)

The jamming transition in the stochastic traffic cellular automaton model of Nagel and Schreckenberg is examined. The behavior of the power spectrum is analyzed. Numerical results are presented. Satisfactory analytical approximations are established in both low frequency and high frequency regions. The intrinsic traffic states are revealed in the middle frequency range. A signature of $1/f$ noise is observed at the critical density of the transition.

DOI: 10.1103/PhysRevE.63.036110 PACS number(s): 89.40.+k, 05.40.Ca, 45.70.Vn

I. INTRODUCTION

The cellular automaton approach to traffic flow has attracted much attention from physicists recently [1]. Instead of equations, the underlying dynamics is governed by a group of update rules applied at discretized time steps. These models are suitable for computer simulations and much numerical work have been reported [2]. Many features observed in real traffic can be captured by a few simple rules. The real time simulation of urban traffic becomes accessible [3]. In contrast, only few analytical results are known [4]. Thus it would be interesting to further study the analytical properties of these cellular automaton models.

The Nagel-Schreckenberg traffic model is essentially a model of traffic flow on a single-lane highway [5]. The main features of traffic flow can be well reproduced, such as the fundamental diagram, backward moving shock waves, and phase separation. As the density increases, traffic jams emerge spontaneously. On crossing a critical density, the transition between free flow and jammed states can be observed, which has been a focus of traffic studies. Several attempts have been made to investigate the properties of the transition, such as using the relaxation time [6], headway distributions [7], density correlations [8], and structure factors [9]. However, it is still not clear whether the transition can be described as a critical phenomenon. In this paper, we study the noise properties of the model by analyzing the power spectrum. Numerical results are presented and analytical approximations are also established.

In the basic model, the road is divided into L cells. Each cell can be either empty or occupied by a car with an integer speed $v \in \{0,1, \ldots, v_{max}\}$, where v_{max} is the speed limit. At each time step, the configuration of N cars is updated by the following four rules, which are applied in parallel to all cars. The first rule is acceleration. If the speed of a car is lower than v_{max}, the speed is advanced by 1. The second rule is slowing down due to other cars. If a car has d empty cells in front of it and a speed larger than d, the speed is reduced to d. The third rule is randomization, which introduces a noise to simulate the stochastic driving behavior. The speed of a moving car ($v \geqslant 1$) is decreased by 1 with a braking probability p. In the fourth rule, the position of a car is advanced by its speed v. Iterations over these simple rules already give realistic results. Real traffic data can be well described by the parameters $v_{max}=5$ and $p=0.5$, where the length of a cell is 7.5m and one time step corresponds to approximately 1 sec [5]. In the following, we will assume these parameters.

II. POWER SPECTRUM

We consider N cars moving on a road of L sites. As a periodic boundary condition is assumed, the global density $\rho=N/L$ is a conserved quantity. We then study the fluctuations of the local density. A small section of the road is designated as the observation post, which has a length of M sites and $M \ll L$. The time series $S(t)$ is recorded as the number of cars on the post at time t. The typical behavior of the time series $S(t)$ is shown in Fig. 1. At small ρ, the local density has only a small fluctuation around its average value, i.e., the global density. At large ρ, the local density can assume a large value as traffic jams emerge. A much larger fluctuation is then observed. The power spectrum $P(\omega)$ is defined by the Fourier transform

$$P(\omega)=\left\langle \left| \frac{1}{T} \sum_{t=1}^{T} S(t) e^{i\omega t} \right|^2 \right\rangle, \tag{1}$$

where $\langle \cdots \rangle$ denotes the average over different initial configurations and $T \gg 1$ is the duration of observation. In this work, a system of $L=10^5$ and $M=20$ is taken. A time series of $T=10^4$ is recorded with the first 10^4 discarded; the average is taken over 10^3 random initial configurations.

A. Low density phase

The typical behavior of the power spectrum at low density is shown in Fig. 2. Oscillations with increasing amplitude are observed in the low frequency region. An abrupt dip followed by a small hump is observed in the high frequency region. In between these two ends, a flat distribution is observed.

In the low frequency region, the power spectrum reveals the long range behavior of the system, which is controlled by the global density ρ. As $\rho \ll 1$, the correlations between cars can be neglected. Thus the cars can be taken as randomly distributed on the road with an expectation value determined by the density ρ. The expectation value of the number of cars within M sites is then given by

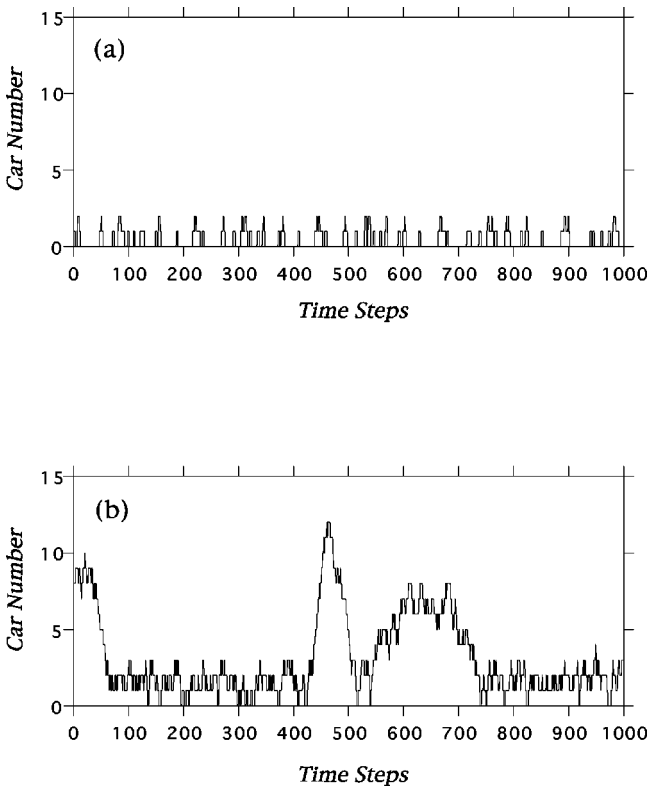

FIG. 1. Time series $S(t)$ at low density $\rho=0.02$ (a) and high density $\rho=0.2$ (b).

$$\langle S(t)\rangle=\sum_{i=0}^{M} iC_i^M\rho^i(1-\rho)^{M-i}=M\rho, \tag{2}$$

where $C_i^M=M!/[i!(M-i)!]$ is the binomial factor. The equal-time correlation is given by

$$\langle S(t)S(t)\rangle=\sum_{i=0}^{M} i^2C_i^M\rho^i(1-\rho)^{M-i}=M\rho+M(M-1)\rho^2; \tag{3}$$

similarly, the different-time correlation is given by

$$\begin{aligned}\langle S(t)\cdot S(t')\rangle&=\sum_{i=0}^{M}\sum_{j=0}^{M} ij[C_i^M\rho^i(1-\rho)^{M-i}]\\&\quad\times[C_j^M\rho^j(1-\rho)^{M-j}]\\&=M^2\rho^2.\end{aligned} \tag{4}$$

Thus the power spectrum is given by

$$\begin{aligned}P(\omega)&=\frac{1}{T^2}\left\langle\left[\sum_{t=1}^{T} S(t)\cos\omega t\right]^2+\left[\sum_{t=1}^{T} S(t)\sin\omega t\right]^2\right\rangle\\&=\frac{1}{T}\langle S(t)\cdot S(t)\rangle+\frac{1}{T^2}\langle S(t)\cdot S(t')\rangle\\&\quad\times\sum_{t\neq t'}(\cos\omega t\cos\omega t'+\sin\omega t\sin\omega t')\end{aligned}$$

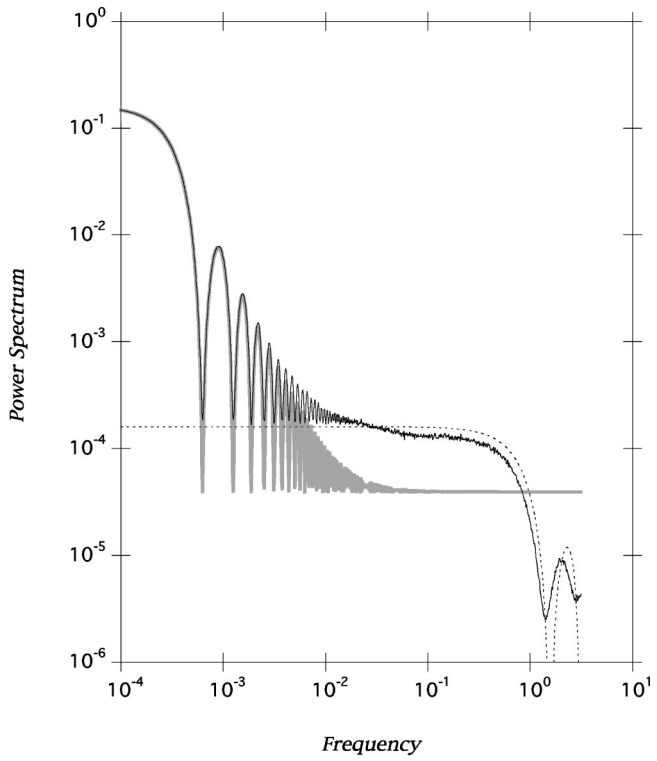

FIG. 2. Power spectrum $P(\omega)$ at low density $\rho=0.02$ (solid line). Analytical approximations for the low frequency region, from Eq. (5), and the high frequency region, from Eq. (9), are shown as the bold gray line and the dotted line, respectively.

$$=\frac{M\rho(1-\rho)}{T}+\frac{M^2\rho^2\sin^2(\omega T/2)}{T^2\sin^2(\omega/2)}. \tag{5}$$

The low frequency part of the numerical results shown in Fig. 2 can be fairly well reproduced by the above analytical expression. In the very low frequency region, $\omega\ll 1/T$, Eq. (5) saturates at a value of $M^2\rho^2$. The amplitude of oscillations is given by $M^2\rho^2/[T^2\sin^2(\omega/2)]$, which increases with decreasing ω; the period of oscillations (in frequency ω) is $2\pi/T$. As the frequency increases, $\omega\geqslant 0.1$, the oscillations diminish and Eq. (5) converges to the value $M\rho(1-\rho)/T$. However, the numerical results show that the spectrum converges to a different value, which can be obtained by the following high frequency approximation.

In the high frequency region, the power spectrum probes the short range behavior of the system, which is then controlled by the length of the observation post M. As the density is low, each car is expected to drive with the maximum speed v_{max}. It takes approximately a time of $t_1=M/v_{max}$ to pass the observation post, i.e., if a car enters the post at time t_0, it leaves the post at time t_0+t_1, and gives a signal

$$S(t)=\begin{cases}1, & t_0<t<t_0+t_1\\ 0 & \text{otherwise.}\end{cases} \tag{6}$$

On average, the temporal separation between two cars is $t_2=1/(\rho v_{max})$. The power spectrum for observing a single car within the time t_2 is then given by

$$P(\omega)=\left[\frac{1}{t_2}\sum_{t=1}^{t_1}\cos\omega(t+t_0)\right]^2+\left[\frac{1}{t_2}\sum_{t=1}^{t_1}\sin\omega(t+t_0)\right]^2; \tag{7}$$

we note that the above distribution is independent of t_0. As the cars are taken to be independent of each other, the power spectrum for a longer time T can be taken as an incoherent sum of the above expression and is given by

$$P(\omega)=\frac{t_2}{T}\left[\frac{1}{t_2}\sum_{t=1}^{t_1}\cos\omega t\right]^2+\frac{t_2}{T}\left[\frac{1}{t_2}\sum_{t=1}^{t_1}\sin\omega t\right]^2. \tag{8}$$

At low frequency, $\omega \ll 1/t_1$, Eq. (8) saturates to a value of $(t_1)^2/(t_2\,T)=M^2\rho/(Tv_{max})$, which reproduces the numerical result. In Fig. 2, we have $M=20$, $v_{max}=5$, and $\rho=0.02$; thus $t_1=4$ and $t_2=10$. The power spectrum reduces to

$$P(\omega)=\frac{2}{5T}[\cos(\omega/2)+\cos(3\omega/2)]^2. \tag{9}$$

The saturated value at low frequency is $8/(5T)$. The dip is located at $\omega=\pi/2\sim 1.57$. The hump is located at $\omega=\cos^{-1}(-2/3)\sim 2.30$ with a height of $P(\omega)\sim 0.119/T$. It is interesting to note that without fine tuning the details, e.g., by considering the effect of random braking, the whole structure in the high frequency part including the location of the dip and the height of the hump can be reproduced quite well.

In summary, the power spectrum at low density ρ can be analytically obtained. In the low frequency region, the observed features are related to the global properties of the system and controlled by the parameter ρ; in the high frequency region, the local properties determine the observed structure and the relevant parameter is M. As we are interested in the transition of traffic states, we shall look into the distributions between these two ends, e.g., $\omega\sim 0.1$ in Fig. 2. As the observation duration T increases, the oscillations in the low frequency region will be shifted to still lower frequency; while the dip and hump in the high frequency region still have the same locations. Thus the power spectrum will be dominated by a flat distribution, which is a characteristic of free flow.

B. High density phase

In contrast, the typical behavior of the power spectrum in the high density phase is shown in Fig. 3. The structures of the dip and hump in the high frequency region can still be observed, but the oscillating behavior at the low frequency region is strongly suppressed. Between these two ends, the power spectrum is significantly enhanced. The flat distribution that characterizes free flow can no longer be observed.

As the density increases, traffic jams begin to emerge. While a car moves forward with various speeds, a well formed jam moves backward with a fixed speed. The enhancement of the power spectrum can be attributed to the appearance of a single wide jam on the road. To simplify the analytical approximation, we assume a number J of cars are crowded bumper to bumper to form a wide jam and the jam

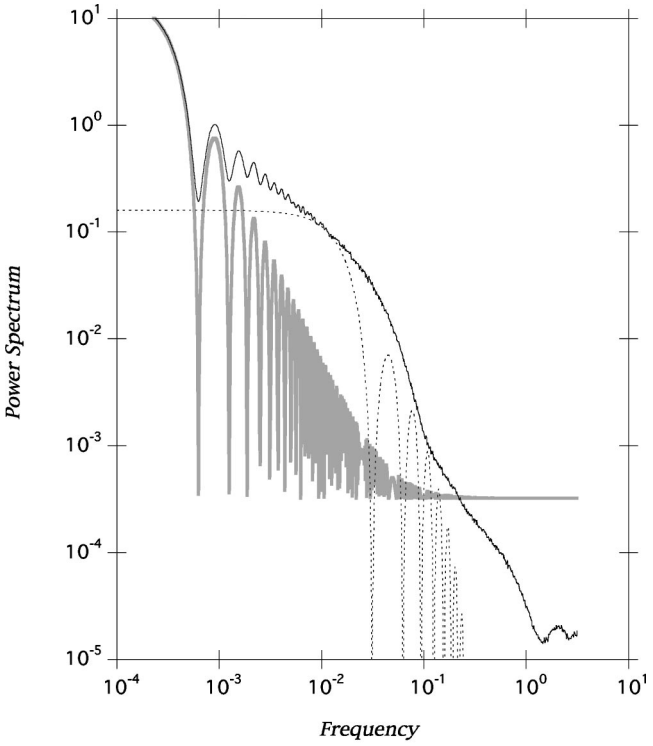

FIG. 3. Power spectrum $P(\omega)$ at high density $\rho=0.2$ (solid line). Analytical approximation for low frequency region is shown as the bold gray line, from Eq. (5). The contribution from a single wide jam of $J=200$ is shown as the dotted line, from Eq. (11).

moves backward with a fixed speed of 1. Then the time series becomes

$$S(t)=\begin{cases} t-t_0, & t_0<t<t_0+M \\ M, & t_0+M<t<t_0+J \\ J+M-t+t_0, & t_0+J<t<t_0+J+M \\ 0 & \text{otherwise,} \end{cases} \tag{10}$$

where t_0 is the time when the jam begins to pass the post, which has a length of M sites. After carrying out the calculation, the power spectrum can be explicitly expressed as

$$P(\omega)=\frac{16}{T^2\omega^4}\sin^2(\omega M/2)\sin^2(\omega J/2). \tag{11}$$

At low frequency, the spectrum saturates to a value of M^2J^2/T^2; at high frequency, it decays like $16\sin^2(\omega M/2)\times(/T^2\omega^4)$, where $J\gg M$ is assumed. In comparison to the random distribution of Eq. (5), the appearance of a wide jam enhances the power spectrum prominently around $\omega\sim\pi/J$ (see Fig. 3). As the length of the jam increases, the enhancement shifts to a lower frequency. In the model, the traffic jam emerges spontaneously and the length of the jam J is not a controlled parameter. With the same global density ρ, the stochastic noise of the model will lead to different sizes of jam even for the same initial configuration. The resulting distribution, shown in the middle region of Fig. 3, can be

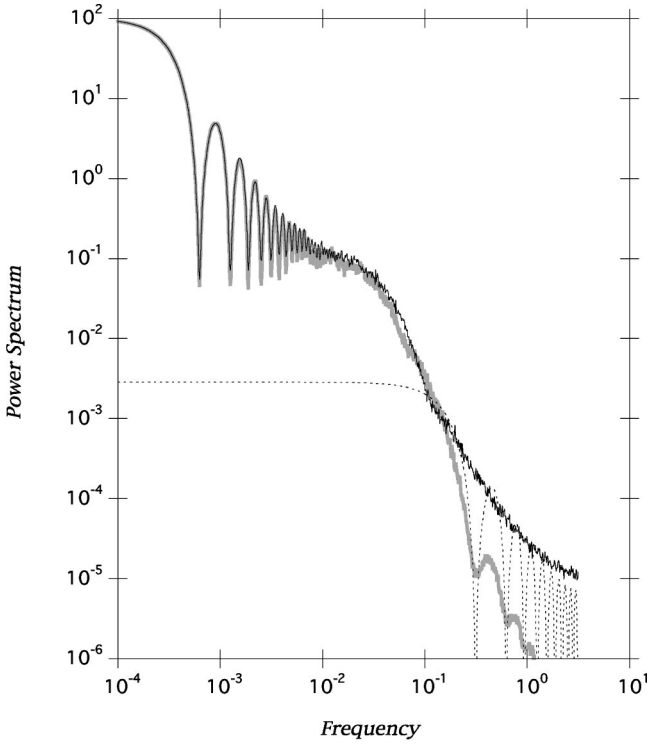

FIG. 4. Power spectrum $P(\omega)$ at high density $\rho=0.5$ (solid line). The result from the multijam approximation is shown as the bold gray line, from Eq. (12). The contribution from free moving cars is shown as the dotted line, from Eq. (14).

taken as an incoherent sum over various weightings of the single-jam result around $J=200$.

In the above approximation, free moving cars are totally neglected. Thus neither the very low frequency limit nor the very high frequency limit of the spectrum can be well described by Eq. (11). As mentioned before, the low frequency limit is solely determined by the global density ρ. Thus the prediction from Eq. (5) is still valid. The saturated value of Eq. (11) will now set a lower cutoff to the oscillating amplitude (see Fig. 3). When one explores the long range properties in the low frequency region, the emergence of a single wide jam will strongly reduce the randomness of the system and thus lead to suppression of the oscillations.

A simple estimation also shows that only a small fraction of cars are within the wide jam. For example, when $\rho=0.2$ and $L=10^5$, only 1% of cars are within the jam of $J=200$; the remaining 99% of cars are still free moving. Thus, when one explores the short range properties in the high frequency region, the characteristic of free flow will still be present, i.e., the structures of dip and bump can still be observed.

As the density ρ further increases, more jams emerge. The oscillations in the low frequency region are somewhat restored; the characteristic of free flow in the high frequency region disappears (see Fig. 4). A multijam configuration becomes essential to have a satisfactory approximation of the power spectrum. Assuming a series of well formed jams moving backward with the same speed, the single-jam formulation in Eq. (11) can be extended to a multijam configuration as follows:

$$P(\omega)=\frac{4}{T^2\omega^4}\sin^2(\omega M/2)\left|\mathcal{N}\sum_{j=1}^{N_j} e^{i\omega t_j}(1-e^{i\omega J_j})\right|^2, \tag{12}$$

where N_j is the number of jams and the index j runs over different jams with length J_j and passing the post at $t=t_j$. A normalization factor $\mathcal{N}$ is introduced to have the correct description of the global density ρ, i.e.,

$$\mathcal{N}=\rho T \Big/ \sum_{j=1}^{N_j} J_j. \tag{13}$$

The saturated value in the very low frequency limit is fixed to reproduce the numerical result. The envelope of oscillations then constitutes a prediction to be compared with the data. Neither the number of jams N_j nor the length of jams J_j is a conserved quantity. With the simple prescription of uniform fluctuations over $\langle N_j\rangle=20$ and $\langle J_j\rangle=500$ at $\rho=0.5$, the typical behavior in Fig. 4 can be fairly well reproduced.

In the above approximation, the underestimation in the very high frequency region is due to the neglect of free moving cars. To estimate the contribution from the free moving cars, we adapt the formulation of the low density results in Eq. (8). As the density increases, the speeds of cars decrease accordingly. The value of t_1, which denotes the time for a car to pass the post, is expected to increase significantly. The power spectrum is then given by

$$P(\omega)=\mathcal{M}\left\{\left[\sum_{t=1}^{t_1}\cos\omega t\right]^2+\left[\sum_{t=1}^{t_1}\sin\omega t\right]^2\right\}$$

$$=\mathcal{M}\frac{\sin^2(\omega t_1/2)}{\sin^2(\omega/2)}, \tag{14}$$

where the normalization factor $\mathcal{M}$ is introduced because only a fraction of cars are moving freely; the dependence on T and t_2 is absorbed into the factor $\mathcal{M}$. With $\mathcal{M}=1/(Tt_2)$, the above formula reduces to Eq. (8). In the low frequency limit, Eq. (14) saturates to a value of $\mathcal{M}(t_1)^2$. In the high frequency region, oscillations with decreasing amplitude are observed. We simply take the average speed to be 1, in contrast to the maximum speed of 5 in the low density case. Then the value of t_1 becomes 20. The factor $\mathcal{M}$ is determined by fixing the data at $\omega\sim0.1$, around which a change of slope is observed. The result is shown in Fig. 4. The envelope of the oscillations matches the data nicely. If one further introduces fluctuations over the speed, an incoherent sum is expected. The rapid oscillations of Eq. (14), resulting from the numerator $\sin^2(\omega t_1/2)$, will be smeared out. The smooth distribution of the data can then be reproduced.

III. DISCUSSION

In this paper, we use the power spectrum to study the noise properties of the Nagel-Schreckenberg traffic model. Besides the numerical work, analytical approximations have also been established. In the low frequency region, the spectrum probes the long range behavior of the system. The most

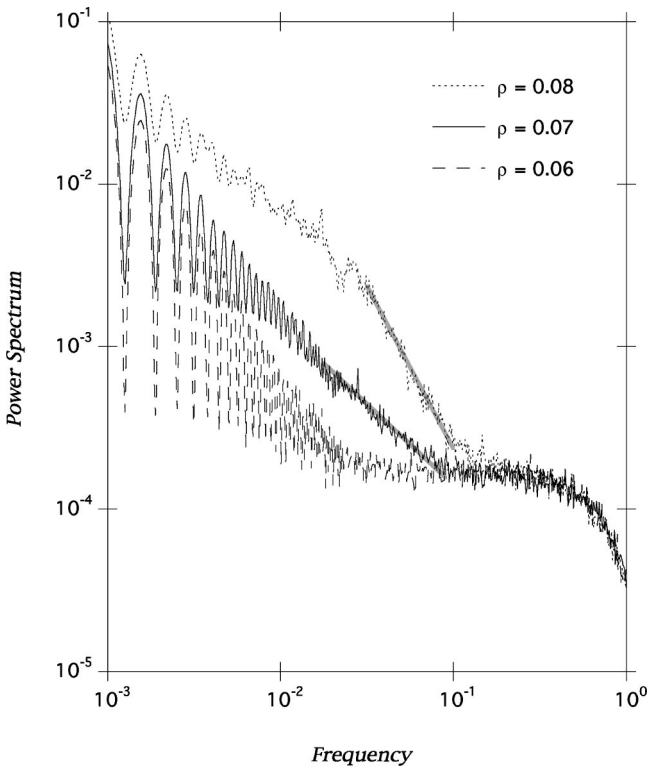

FIG. 5. Power spectrum $P(\omega)$ for various values of density. The characteristic slopes of -1 and -2 are marked by bold gray sections.

important parameter is the density ρ. In the very low frequency limit, $\omega \leqslant 10^{-4}$ in a system of $L=10^5$, the spectrum saturates to a value of $M^2\rho^2$. As the frequency increases, oscillating behavior is observed. When the density is low, the oscillations can be attributed to the randomness of the free moving cars. As the density increases, a traffic jam begins to emerge. Around the onset of the traffic jam, the first wide jam to emerge significantly reduce the randomness of the system. Thus the oscillating behavior diminishes accordingly. As the density increases further, the number of jams also increases. The randomness of the system is then enhanced. The restored oscillating behavior is now attributed to the randomness of the multijam configurations. The frequency dependence of these features is directly related to the system size. As the system size increases, the saturated frequency decreases and the oscillating behavior shifts to a lower frequency. Thus for an infinite system such oscillating behavior can be neglected.

In the high frequency region, the spectrum reveals the short range behavior of the system. The most important parameter becomes the length of the post M, which provides a cutoff and results in a more rapid drop of the spectrum. When the density is low, the speed is high. A car passes the post within a short time and leaves a short pulse to be observed, which results in the interesting signature of the dip and hump. As cars drive at the speed limit, the variation of speeds can be neglected. The signals of dip and hump from different cars are superimposed and become a clear signature of the power spectrum in the low density phase. As the density increases, the speed decreases and the observed pulse elongates. The signal of dip and hump appears at a lower frequency. However, the variation of speeds becomes significant and the structure of dip and hump is smeared out; thus a monotonic decrease of the spectrum results in the high density phase. These features are mainly controlled by the length of the post M and are independent of the system size L. As the system size increases, these features can be observed at the same frequency.

The low and high frequency regions of the power spectrum reveal structures on the scales L and M, respectively. However, we are interested in the intrinsic traffic states that should be revealed in the middle frequency range, i.e., around $\omega \sim 10^{-1}$ for a system of $L=10^5$. When the density is low, a flat distribution is observed, which can be taken as white noise characterizing the free flow. When traffic jams emerge as the density increases, the power spectrum is enhanced predominantly at the low frequency end, while the high frequency end remains unchanged. Thus the flat distribution becomes a steeper drop and $1/\omega^2$ dependence is observed, which characterizes the jammed states. As the density increases, the slope of the power spectrum changes from 0 to -2, which characterize the randomness of free moving cars and well formed jams, respectively. It is interesting to note that the change of slope is not gradual, but occurs suddenly at a critical density. The ρ dependence of the power spectrum is shown in Fig. 5. A clear signature of $1/\omega$ dependence, also known as $1/f$ noise, is observed at the critical density. In this work, the observed $1/f$ noise is sustained only for a decade of the frequency (see Fig. 5). However, from the above analysis, it should be clear that the $1/f$ noise will become the dominant signature if one further increases the system size. The value of critical density obtained, $\rho \sim 0.08$, is consistent with that from other approaches. We expect this signature could be used as a convincing definition of the transition between free flow and jammed states. $1/f$ noise occurs widely in many other systems and is considered to be a mysterious phenomenon. In addition to traffic related problems, further research into the Nagel-Schreckenberg traffic model may lead to a more precise understanding of systems exhibiting $1/f$ noise.

[1] D. Chowdhury, L. Santen, and A. Schadschneider, Phys. Rep. **329**, 199 (2000).

[2] For example, see *Traffic and Granular Flow '99*, edited by D. Helbing, H. J. Herrmann, and M. Schreckenberg (Springer Verlag, New York, 2000).

[3] M. Rickert and K. Nagel, Int. J. Mod. Phys. C **8**, 483 (1997); K. Nagel and C. L. Barrett, *ibid.* **8**, 505 (1997); J. Esser and M. Schreckenberg, *ibid.* **8**, 1025 (1997).

[4] A. Schadschneider, Eur. Phys. J. B **10**, 573 (1999).

[5] K. Nagel and M. Schreckenberg, J. Phys. I **2**, 2221 (1992); M.

Schreckenberg, A. Schadschneider, K. Nagel, and N. Ito, Phys. Rev. E **51**, 2939 (1995).

[6] M. Sasvári and J. Kertész, Phys. Rev. E **56**, 4104 (1996); B. Eisenblätter, L. Santen, A. Schadschneider, and M. Schreckenberg, *ibid.* **57**, 1309 (1998).

[7] D. Chowdhury, A. Pasupathy, and S. Sinha, Eur. Phys. J. B **5**, 781 (1998); D. Chowdhury, L. Santen, A. Schadschneider, S. Sinha, and A. Pasupathy, J. Phys. A **32**, 3229 (1999).

[8] S. Cheybani, J. Kertész, and M. Schreckenberg, J. Phys. A **31**, 9787 (1998); L. Neubert, H. Y. Lee, and M. Schreckenberg, *ibid.* **32**, 6517 (1999).

[9] S. Lübeck, M. Schreckenberg, and K. D. Usadel, Phys. Rev. E **57**, 1171 (1998); L. Roters, S. Lübeck, and K. D. Usadel, *ibid.* **59**, 2672 (1999).